Am J Physiol Heart Circ Physiol 307: H910–H921, 2014.
First published July 18, 2014; doi:10.1152/ajpheart.00332.2014.

An afferent explanation for sexual dimorphism in the aortic baroreflex of rat

Grace C. Santa Cruz Chavez,[1,2] Bai-Yan Li,[2] Patricia A. Glazebrook,[3] Diana L. Kunze,[3,4] and John H. Schild[1,2]

[1]*Stark Neurosciences Research Institute, Indiana University School of Medicine, Indianapolis, Indiana;* [2]*Department of Biomedical Engineering, Indiana University Purdue University Indianapolis, Indianapolis, Indiana;* [3]*Rammelkamp Center for Education and Research, MetroHealth Campus, Cleveland, Ohio; and* [4]*Department of Neurosciences, Case Western Reserve University, Cleveland, Ohio*

Submitted 19 May 2014; accepted in final form 14 July 2014

Santa Cruz Chavez GC, Li BY, Glazebrook PA, Kunze DL, Schild JH. An afferent explanation for sexual dimorphism in the aortic baroreflex of rat. *Am J Physiol Heart Circ Physiol* 307: H910–H921, 2014. First published July 18, 2014; doi:10.1152/ajpheart.00332.2014.—Sex differences in baroreflex (BRx) function are well documented. Hormones likely contribute to this dimorphism, but many functional aspects remain unresolved. Our lab has been investigating a subset of vagal sensory neurons that constitute nearly 50% of the total population of myelinated aortic baroreceptors (BR) in female rats but less than 2% in male rats. Termed "Ah," this unique phenotype has many of the nonoverlapping electrophysiological properties and chemical sensitivities of both myelinated A-type and unmyelinated C-type BR afferents. In this study, we utilize three distinct experimental protocols to determine if Ah-type barosensory afferents underlie, at least in part, the sex-related differences in BRx function. Electron microscopy of the aortic depressor nerve (ADN) revealed that female rats have less myelin ($P < 0.03$) and a smaller fiber cross-sectional area ($P < 0.05$) per BR fiber than male rats. Electrical stimulation of the ADN evoked compound action potentials and nerve conduction profiles that were markedly different ($P < 0.01$, $n = 7$ females and $n = 9$ males). Selective activation of ADN myelinated fibers evoked a BRx-mediated depressor response that was 3–7 times greater in female ($n = 16$) than in male ($n = 17$) rats. Interestingly, the most striking hemodynamic difference was functionally dependent upon the rate of myelinated barosensory fiber activation. Only 5–10 Hz of stimulation evoked a rapid, 20- to 30-mmHg reduction in arterial pressure of female rats, whereas rates of 50 Hz or higher were required to elicit a comparable depressor response from male rats. Collectively, our experimental results are suggestive of an alternative myelinated baroreceptor afferent pathway in females that may account for, at least in part, the noted sex-related differences in autonomic control of cardiovascular function.

baroreceptor; cardiovascular; vagal; autonomic nervous system; visceral

THE ARTERIAL BAROREFLEX (BRx) is essential for robust regulation of cardiovascular function. Rapid BRx-mediated adjustments in heart rate (HR) and arterial blood pressure (BP) are achieved by altering autonomic outflow to the heart and blood vessels (31, 59, 67). Such BRx responses are dynamically modulated by the pressure-dependent discharge of arterial baroreceptor (BR) afferents that provide a continuous stream of systemic hemodynamic information to the central nervous system and are therefore essential to maintaining cardiovascular homeostasis (1, 10, 26). Recent and emerging studies document sex-related differences in many clinical assessments of integrated BRx function (3, 6, 8, 13, 16, 36, 37, 44, 57). Often, such differences are interpreted relative to sex-specific hormonal regulation of autonomic control (15, 19, 22, 68). However, the underlying mechanisms and physiological significance of such hypotheses derived from both human and experimental animal preparations remain discordant (43, 51, 71, 72).

Recent cellular electrophysiological studies of BR afferent function in rat have led us to consider alternative hypotheses regarding the origins of sexual dimorphism in BRx function (48, 60). In female rats, there exists two functionally distinct and comparably sized populations of myelinated BR afferents termed A- and Ah-type (~50% each). In stark contrast, there exists only a single and far more homogeneous population of A-type myelinated barosensory afferents (~98%) in male rats. This is highly significant because BRx modulation of integrated autonomic control of cardiovascular function is closely associated with the neural encoding properties of myelinated as well as unmyelinated barosensory afferents (21, 25, 41, 66). Differences in the distribution of myelinated barosensory afferents between the sexes may account for, at least in part, the observed sexual dimorphism in BRx function and may well represent a novel and as yet unrecognized afferent mechanism underlying the noted sex differences in cardiovascular regulation (38). However, definitive experimental evidence is lacking.

The in situ study of the rat aortic BRx has proven to be a particularly useful experimental preparation for elucidating the disparate reflexogenic function of myelinated and unmyelinated barosensory afferents (24, 26, 55). This is because in the rat BR axons arising from the aorta assemble into a readily identifiable and purely mechanosensory afferent fiber bundle termed the aortic depressor nerve (ADN), the activation of which initiates a rapid reduction in HR and BP solely via the aortic BRx (45, 55, 63). Barosensory fibers of the ADN have long been classified as either myelinated A-type afferents with diameters in the range of 1–7 μm or unmyelinated C-type afferents with diameters in the range of 0.25–1.5 μm (9, 27, 28). Due to widely known differences in fiber anatomy and ion channel distributions (58, 64), myelinated A-type barosensory afferents have an electrical activation threshold well below that of unmyelinated C-type barosensory afferents. Similar differences enable low-threshold myelinated A-type BR fibers and neurons to sustain repetitive discharge rates well in excess of 50 Hz, while the higher threshold unmyelinated C-type BR fibers and neurons typically function at much lower rates and not often with steady or sustained discharge beyond ~20 Hz (49). Interestingly, the threshold and dynamic discharge characteristics of the additional population of myelinated Ah-type

Address for reprint requests and other correspondence: J. H. Schild, Dept. of Biomedical Engineering, Indiana Univ. Purdue Univ. Indianapolis, 723 W. Michigan St., SL 220, Indianapolis, IN 46202 (e-mail: jschild@iupui.edu).

BR afferents in female rats fall well within the range bounded by what are essentially two, nonoverlapping distributions of electrophysiological properties associated with myelinated A-type and unmyelinated C-type BR afferents (48, 50, 60). A similar bimodal distribution is evident in the frequency-dependent reflex integration of A- and C-type barosensory afferents in male rats (24, 26). For example, a rapid reduction of 20–30 mmHg can be elicited either through selective electrical activation of myelinated A-type BR fibers but only at sustained rates of nerve discharge of 50 Hz or higher. In stark contrast, selective activation of unmyelinated C-type BR afferents can elicit a comparable depressor response at nerve stimulation rates below 10 Hz.

As the population of myelinated Ah-type BR afferents in male rats may be too small (<2%) to be of functional significance, in situ BRx studies were carried out using a cohort of aged-matched female and male rats. Experimental objectives were *1*) to quantify the functional recruitment of Ah-type barosensory afferent fibers in the left ADN and *2*) to determine what, if any, impact this additional pathway of myelinated barosensory afferents may have upon the frequency-dependent integration of the BRx. Collectively, our results support the hypothesis that low-threshold myelinated Ah-type aortic BR afferents substantially enhance the initial depressor response of the BRx in female compared with male rats and that these functional differences may account for, at least in part, the enhanced parasympathetic control of BP in females (3, 44).

MATERIALS AND METHODS

All animal use protocols were approved by the Institutional Animal Care and Use Committee of the Purdue School of Science, Indiana University Purdue University Indianapolis (IUPUI) or the School of Medicine, Case Western Reserve University. All protocols involved blunt dissection through the superficial and underlying musculature of the neck cavity under stereomicroscopy (×40) to expose the left ADN for further microsurgical manipulation and experimentation (48). An intraperitoneal injection of a ketamine/xylazine (0.1 ml/100 g) anesthetic was used in the histological and electrophysiological preparations while an intraperitoneal injection (0.8 ml/100 g) of a combination of urethane (800 mg/kg; Acros Organics, NJ) and α-chloralose (80 mg/kg; Fisher Scientific, Pittsburgh, PA) was used for in situ study of the aortic BRx. No attempt was made to assess or control for the phase of estrous cycle in female rats.

Electron microscopic study of the ADN. The left ADN from age-matched cohorts of female ($n = 7$) and male ($n = 7$) rats was prepared for electron microscopic (EM) study. A sample of nerve tissue at approximately 5–8 mm caudal to the 10th cranial (vagal) ganglion was excised, pinned to a rubber substrate, and immediately immersed in a room temperature PBS solution containing 3% paraformaldehyde and 1% glutaraldehyde for 1 h. The sample was then stored overnight at 4°C in a PBS solution containing only 3% paraformaldehyde. The tissue was then postfixed with 1% osmium tetroxide and 1% potassium ferricyanide followed by alcohol dehydration of 25–100% that included en bloc staining in 1% uranyl acetate. This was followed by immersion in 100% alcohol and propylene oxide for 20 min followed by three changes of propylene oxide. The embedding protocol proceeded overnight with the specimens rotating with a mixture of propylene oxide with epon-araldite in a 1:1 ratio, followed by a 4- to 6-h treatment with epon-araldite alone. These prepared nerve samples were embedded in blocks with fresh epon-araldite and cured overnight at 70°C. The samples were sectioned to 90 nm using an ultramicrotome MT-X (RMC, Tucson, AZ) and mounted on formvar/carbon-coated 100-mesh copper grids. Following poststaining with 1% uranyl acetate and Reynolds's lead stain, the grids were imaged (15,000×, 80 kV) using a Tecnai G2 transmission electron microscope (FEI, Hillsboro, OR) equipped with an AMT digital camera. Digital images of each EM section were montaged for reconstruction of the entire cross-section of the left ADN using system software and later delimited to an eight-bit grayscale using ImageJ (65). A common threshold adjustment was made to delineate the external and internal edges of the myelin sheath from surrounding tissues which also circumscribed the central axon. A pixel count (μm^2/pixel) made possible a calculation of the total area (μm^2) of both the myelin sheath and the central axon for each myelinated BR nerve fiber. From these two data estimates, the myelin sheath thickness, equivalent circular diameters of the axon and BR fiber, and the g-ratio, i.e., ratio of the inner axonal diameter to the total outer diameter of the myelinated BR fiber, could be resolved.

Electrophysiological study of the ADN. The left ADN from age-matched cohorts of female ($n = 7$) and male ($n = 9$) rats was prepared for a stimulus recording protocol using a neurosurgical stereo microscope (F40 model M520, Leica Microsystems, Burr Ridge, IL). An orthogonal arrangement of the anode and cathode pairs for each bipolar electrode (800-μm anode/cathode spacing, FHC, Bowdoin, ME) provided a more uniform field potential about the bipolar recording electrode and greatly reduced the stimulus artifact. The bipolar stimulation electrode was positioned close to the point of entry of the ADN into the chest cavity but well before any significant branching of the nerve trunk. The bipolar recording electrode was typically 20 mm rostral to the stimulation electrode and ~5 mm from the 10th cervical (vagal) ganglion. All separation distances were measured using a digital caliper (Marathon, Richmond Hill, Ontario, Canada). The ADN was then transected at both ends and covered with a mixture of petroleum jelly and mineral oil. A stimulus recording paradigm (iWorx, Dover, NH) acquired a running average of 25 200-ms epochs of amplified and band-pass filtered evoked nerve activity (×50 to ×100 K, 1–5,000 Hz). Regulated 200-μs monophasic voltage pulses ranging from 0.1 to 20.0 V in magnitude were delivered to the ADN once per second (Iso-flex, A.M.P.I., Jerusalem, Israel). A ratio of the separation distance between the stimulation and recording electrodes and the time interval between the stimulus artifact and the leading edge of the synchronized voltage deflections of a traveling CAP has long provided a reliable measure of fiber conduction velocity (CV, m/s) even in small-diameter, Group III (<5 μm) myelinated afferents (7). Those CAP deflection profiles traveling at >10 m/s were classified as myelinated, A-type afferents (Group III, Aαβ fibers), while those CAP traveling at speeds <10 m/s but >2 m/s were classified as myelinated, Ah-type afferents (Group III, Aδ fibers). Those synchronized voltage deflections arriving late in the recording epoch and traveling below 2 m/s were presumed to arise from unmyelinated BR fibers. Through such indexing the average signal power, i.e., energy per unit time arising from each distinct traveling CAP, could be quantified as a root mean square value (RMS). Significant differences in the RMS magnitude of the CV-indexed CAP would be consistent with meaningful differences in the relative numbers of myelinated A- and Ah-type aortic BR fibers between female and male rats.

Graded electrical stimulation of the ADN and baroreflex dynamics. Age-matched cohorts of female ($n = 16$) and male ($n = 17$) rats were used for in situ study of the aortic BRx. A ventral midline incision was made along the neck musculature to expose the trachea for cannulation to facilitate spontaneous respiration of room air. The left femoral artery was exposed and catheterized using a short length (10 mm) of PE-10 tubing filled with heparinized saline (30 U/ml). Calibrated voltage transduction (Radnoti, Monrovia, CA) of arterial blood pressure was low-pass filtered at 500 Hz and digitized at 1 kHz using LabVIEW (National Instruments, Austin, TX). Microsurgical placement of the bipolar stimulation electrode was carried out as described above.

BRx protocols proceeded once the mean arterial blood pressure (MAP) stabilized to within 10% of the target baseline of 100 mmHg,

defined here as "resting" MAP. This was generally achieved within 15–30 min following final placement of the stimulation electrode. Constant-voltage monophasic pulses from 1 to 5 V in 0.5-V increments and 6, 8, 10, 12, 15, 18, and 20 V in magnitude were used to test for a depressor response. Each was tested at rates of 1, 2, 5, 10, 20, 30, 50, 75, and 100 Hz for a total of 144 unique combinations of stimulus intensity and frequency. A single, unique pair of stimulus magnitude and stimulus rate was randomly selected without replacement from this combined set of stimulus parameters and applied for a duration of 30 s. Subsequent trials were not initiated until femoral pressure recovered to resting MAP, typically within 1–2 min. A stable MAP was often well maintained for at least the first 120 min, but this limited recordings to only a subset of randomly selected pairs of intensity and frequency. For those experimental protocols extending beyond 120 min, a supplemental intraperitoneal injection of urethane and α-chloralose (10% of initial dosage) was often required to maintain a stable resting MAP. The experiment was terminated if femoral pressure failed to recover to resting MAP within 5 min.

Analysis of data. All averaged data are presented as means ± SD with differences noted as significant at $P < 0.05$. Raw measures of myelin and axon area were used to derive estimates of several widely studied anatomical features of myelinated nerve. These derived sample measurements, or data replicates, were analyzed using a nested ANOVA (SPSS, IBM, Armonk, NY) to assess statistical significance. Statistical comparison of RMS magnitudes of CV-indexed CAP between male and female groups was carried out in SPSS using an independent *t*-test and Levene's test for equality of variances. The average of a 1-s epoch of femoral pressure about the peak depressor response was divided by the average of a 10-s sample of raw arterial pressure measured just prior to the start of nerve stimulation. Multiplied by 100, this quotient quantified the peak change in femoral pressure (ΔMAP) relative to the resting MAP with significance assessed as with the RMS data. Heart rate at both resting MAP and peak ΔMAP was calculated offline through a Fourier spectral analysis of each raw BP recording (Matlab 2011b, Mathworks).

RESULTS

We investigated a compendium of neuroanatomical, electrophysiological, and reflexogenic properties associated with the left ADN of adult female (266 ± 31 g, $n = 33$) and adult male (394 ± 41 g, $n = 30$) Sprague-Dawley rats (Harlan, Indianapolis, IN), 12–18 wk of age.

Sexual dimorphism in myelinated aortic baroreceptor fibers: neuroanatomical evidence. Cross-sections of the left ADN revealed female rats ($n = 7$, 16 wk, 283 ± 49 g) had a significantly smaller diameter nerve trunk (32.7 ± 5 vs. 42.4 ± 6 μm, $P < 0.01$) than male rats ($n = 7$, 16 wk, 386 ± 18 g). Female rats had a greater number of myelinated fibers on average per nerve trunk compared with male rats (61 ± 18 vs. 49 ± 25). A serial montage of these high-resolution nerve sections enabled precise measurement of myelin and axon area (μm^2) from a large sample of fibers from female and male rats: 425 and 344 fibers, respectively (Fig. 1). From these two measures, several estimates of myelinated nerve anatomy were shown to be statistically significant [female (F) vs. male (M), $P < 0.05$]: myelin area, 3.02 ± 2.1 vs. 3.68 ± 5.8 μm^2; myelin thickness: 0.94 ± 0.4 vs. 1.01 ± 0.5 μm; fiber area, 4.75 ± 3.39 vs. 5.71 ± 9.25 μm^2; and fiber diameter, 2.33 ± 0.8 vs. 2.45 ± 1.1 μm. Additional calculated measures for axon area (1.73 ± 1.5 vs. 2.04 ± 3.5 μm^2) and g-ratio (0.60 ± 0.1 vs. 0.59 ± 0.1) were not significantly different. Frequency histograms for measures of myelin and fiber area were approximately unimodal with no compelling differences in the distribution of these population profiles (Fig. 1). However, a notable exception was the variance (σ^2) in the distribution of myelin area, which was eightfold broader in males compared with females ($\sigma^2 = 33.63$ vs. 4.41). This may be due, at least in part, to the occasional occurrence of one larger-diameter (8–12 μm)

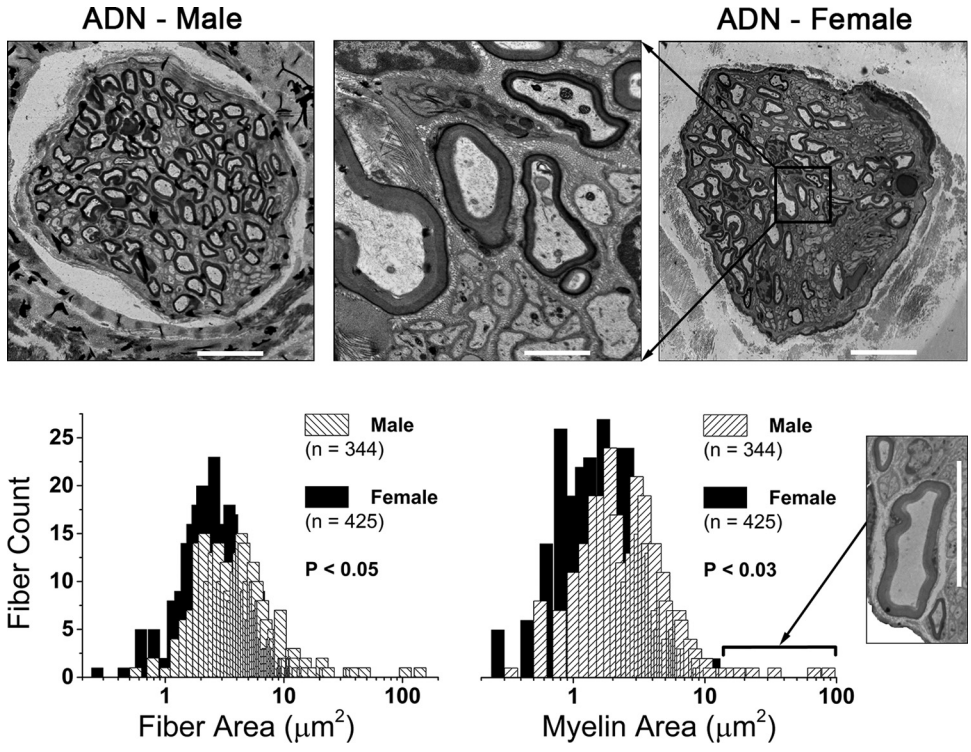

Fig. 1. Sexual dimorphism in the myelination of rat aortic baroreceptor (BR) fibers. Top panels: electron microscopy images of the left aortic depressor nerve (ADN) from an adult male and female rat. Scale bars represent 10 μm and 1.5 μm for low and high (middle panel) magnification, respectively. Bottom panels: frequency distribution of fiber (axon + myelin) and myelin cross-sectional area (μm^2). These two neuroanatomical features were the most significantly different across the populations of ADN myelinated fibers from female ($n = 7$) and male ($n = 7$) rats, with both measurements being significantly smaller in females. Bin centers increment in steps of 0.2 μm. *Inset*: several male nerve trunks contained at least one large myelinated BR fiber with axon and myelin area that were 5–10 times greater than population averages. Such large-diameter fibers were not observed in the ADN of female rats. Scale bar for inset is 10 μm.

myelinated fiber in the left ADN of male rats (Fig. 1, *inset* near myelin histogram). Only 3 of these larger-diameter myelinated fibers were among the 344 myelinated fibers analyzed from male rats, and although these few data slightly skewed the average toward larger values of myelin and fiber area, their removal from the data set did not alter statistical significance. No such large-diameter myelinated fibers were observed in the left ADN of female rats.

Sexual dimorphism in myelinated aortic baroreceptor fibers: electrophysiological evidence. Fiber area and myelin thickness are well known to be reliably correlated with electrical threshold for fiber discharge and CV (78). Therefore, in situ electrophysiological studies were carried out to determine if the observed differences in fiber and myelin area also present as quantitative differences in the electrically evoked CAP from the left ADN of male ($n = 9$, 16 wk, 419 ± 41 g) and female ($n = 7$, 17 wk, 279 ± 10 g) rats. Stable, low-noise CAP with a modest stimulus artifact could be reliably recorded with as little as 15-mm spacing between the stimulus and recording electrodes (Fig. 2). At stimulus intensities as low as 0.1–0.3 V, recruitment of the lowest-threshold and presumably largest A-type myelinated fibers presented as a distinct CAP, separate and delayed relative to the stimulus artifact. The CV of these fibers was estimated to be in the range of 60 m/s for males and 50 m/s for females but were not significantly different. Myelinated fibers with slightly higher electrical thresholds and presumably smaller diameters were recruited at 0.5–1.0 V, which increased the complexity of the CAP within an epoch consistent with fiber CV in the range of 20 m/s for males and 15 m/s for females. Although not statistically different, this range of fiber CV is consistent with the continued recruitment of faster-conducting and larger-diameter myelinated A-type fibers in both male and female rats. Use of a finer gradation in stimulation intensities provided an opportunity to quantify the root mean square (RMS) magnitude of the CAP signal energy as a function of stimulus intensity. The recruitment profiles for these lowest-threshold and presumably largest-diameter myelinated A-type fibers were remarkably similar between male and female rats (Fig. 3). The A-volley CAP from both sexes exhibited an asymptotic increase in RMS magnitude with increasing stimulus intensity that plateaued around 1.25–1.75 V and remained within 14% of this stable magnitude through to 5 V of bipolar nerve stimulation (Fig. 3*A*, gray arrow). Also starting at ~0.5 V of stimulation there was a distinct CAP volley in female rats that was quite delayed in time from the nerve stimulus and presumably related to the recruitment of the smaller-diameter, myelinated Ah-type fibers with CV at or below 10 m/s (Fig. 2). This delayed CAP was not well represented in any of the nerve recordings from male rats. In female rats, starting at 0.4 V of stimulation the average RMS magnitude of this delayed CAP was significantly ($P < 0.05$) greater than the RMS of the corresponding epoch from male rats (Fig. 3*B*), which failed to exhibit any obvious indication of a well-defined, repeatable afferent volley (Fig. 2). Further increases in stimulus intensity brought about a near-linear increase in the RMS magnitude of the delayed CAP in female rats that showed signs of saturation, starting just beyond 1.0 V of stimulation. Further increases in stimulation intensity through

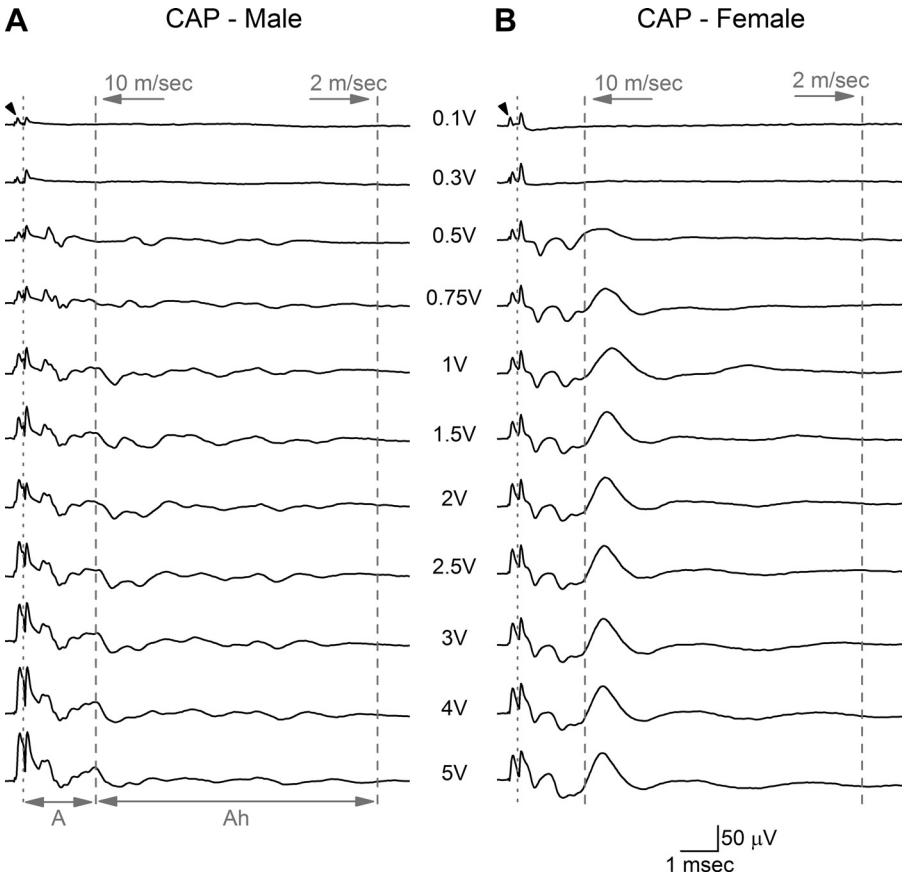

Fig. 2. Representative compound action potentials (CAP) from the left aortic depressor nerve (ADN) of male and female rats. Bipolar, constant-voltage stimulation (arrowhead) of the ADN in a male (*A*) and a female (*B*) rat showed clear differences in the magnitude and timing of the CAP evoked from low-threshold myelinated baroreceptor (BR) afferent fibers. The CAP corresponding to the faster-conducting A-type fibers was discernable at stimulation intensities as low as 0.1 V. The leftmost dotted line separates the stimulus artifact from the leading edge of the CAP for A-type fibers which extends through to the 10-m/s demarcation (dashed line). The CAP corresponding to the slower-conducting Ah-type fibers was bounded by the 10-m/s and 2-m/s demarcation lines. The CAP for the Ah-type BR fibers was apparent at low stimulus intensities (~0.5 V) in female rats, but in male rats no such Ah-type volley was observed. Each trace is an average of 25 recordings at a stimulus rate of 1 Hz.

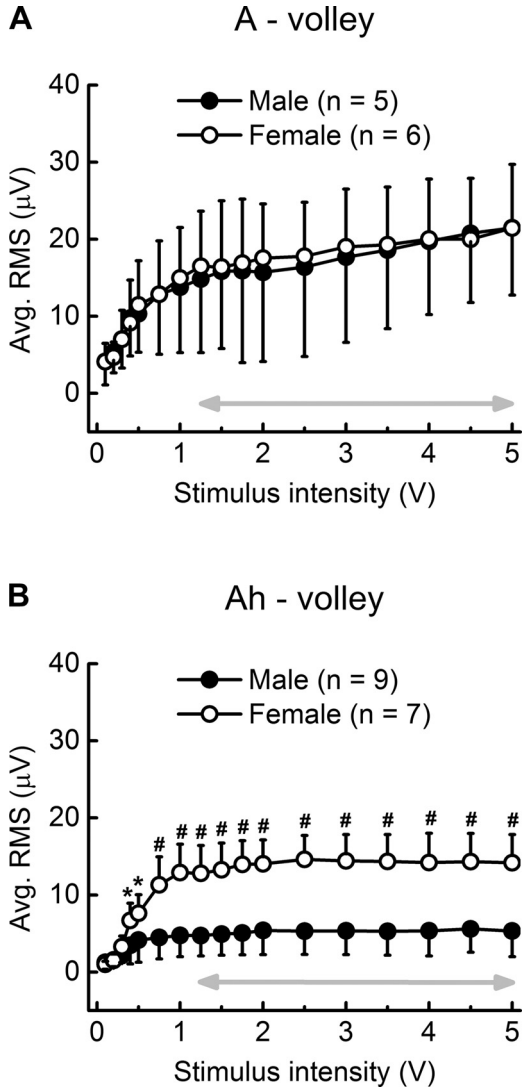

Fig. 3. Average integrated magnitude (RMS) of the CAP from low-threshold myelinated A- and Ah-type baroreceptor fibers as a function of stimulus intensity. *A*: the RMS of the CAP from A-type fibers in male and female rats was remarkably similar. *B*: in stark contrast, the RMS of the CAP from Ah-type fibers in female rats was significantly greater than those from male rat over all but the lowest stimulation intensities (<0.5 V). Double arrow highlights the range of suprathreshold activation, i.e., a CAP of constant magnitude and yet increasing stimulation intensity. Both populations of low-threshold A- and Ah-type fibers exhibited graded recruitment at only the lowest stimulus intensities (less than ~0.5 V). Data are means ± SD. *$P < 0.05$, #$P < 0.01$.

to 5 V brought about a remarkably stable plateau in the RMS magnitude of the CAP from Ah-type fibers (≤1% variation) that was significantly ($P < 0.01$) greater than the less synchronized, smaller-magnitude response observed from male rat (Figs. 2 and 3*B*). Such stability in the RMS magnitude of the CAP from Ah-type fibers is presumably a consequence of the complete electrical recruitment of all low-threshold, myelinated BR fibers in the left ADN starting at ~1.25 V of bipolar stimulation (Fig. 3, gray arrows).

At stimulus intensities beyond 5 V, a broad and less well-defined CAP begins to appear late in the nerve recording from both sexes. These smaller-magnitude and slower-conducting CAP complexes presumably represent the recruitment of high-threshold, unmyelinated C-type fibers with axon diameters considerably smaller than myelinated BR fibers and with CV of <2 m/s (Fig. 4*A*). At the maximum stimulation intensity tested, the average magnitude of the CAP from these C-type fibers was never much greater than 5 μV RMS with remarkable similarity in the recruitment profiles from male and female rats (Fig. 4*D*). Such low-magnitude and desynchronized responses from these high-threshold, slowest-conducting unmyelinated fibers were in stark contrast to the more synchronized CAP arising from myelinated BR fibers. In female rat, the plateau exhibited in the RMS magnitude of the Ah-fiber CAP at low stimulation voltages was sustained through to 20 V of stimulation and remained significantly ($P < 0.01$) greater than the corresponding measure from male rats (Fig. 4*C*, gray arrow). Interestingly, in male rats the average RMS magnitude of the Ah-fiber CAP never exceeded the average RMS for the CAP of unmyelinated fibers from either sex. The faster-conducting myelinated A-type fibers exhibited a plateau in CAP magnitude from about 1.25–5 V of bipolar stimulation that was followed by a near-linear increase in the average RMS magnitude as stimulus intensity approached 20 V. This was a consequence of the increasing stimulus artifact that extended into the epoch for measuring the CAP arising from these faster-conducting myelinated A-type fibers (Fig. 4*B*, note *inset* and upward inflection of gray arrow).

Sexual dimorphism in the baroreflex: functional evidence from the selective recruitment of low-threshold, myelinated aortic baroreceptor fibers. In situ BRx studies were carried out to determine whether the electrical recruitment of low-threshold, myelinated BR fibers in female ($n = 16$, 14 wk, 254 ± 22 g) and male ($n = 17$, 14 wk, 384 ± 43 g) rats revealed evidence of sexual dimorphism in the reflex response, as might be inferred from the in situ nerve recordings (Figs. 2–4). Femoral BP was monitored throughout each experiment, and the average resting MAP and HR were calculated for female and male rats (92.4 ± 7.9 vs. 100 ± 9.2 mmHg and 394 ± 33.6 vs. 381 ± 29.3 beats/min, respectively). Once the ADN was dissected away from the vagus and surrounding tissues, it was placed on a bipolar hook electrode. An abrupt and sustained depressor response that peaked within 2–4 s from the start of a 50-Hz burst of 3-V pulses confirmed that the hooked nerve was the left ADN. For the raw BP traces presented in Fig. 5, a bipolar stimulus magnitude of 1.5 V was utilized as this had been shown to effectively recruit all myelinated BR fibers in the left ADN of both sexes as well as being far below the minimum electrical threshold for unmyelinated C-type afferent fibers (Fig. 4). Increasing the rate of the 1.5-V stimulation clearly demonstrated a robust frequency-dependent reduction in the MAP along a time course that was qualitatively similar between male and female rats. However, markedly lower rates of nerve stimulation were required to evoke a rapid, 20- to 30-mmHg depressor response in female compared with male rats. Indeed, in female rats a clear depressor response was reliably produced by 1.5-V pulses at stimulation rates as low as 5 Hz, whereas in male rats the first evidence of a reduction in MAP does not occur until 20–30 Hz of repetitive stimulation (see Fig. 5, *A* and *B*; compare highlighted traces).

The remaining studies were carried out to determine if such a functional bias was preserved across the 0.1- to 5.0-V stimulation magnitudes that are almost entirely associated with the selective recruitment of low-threshold, myelinated BR afferents (Figs. 2–4). At a stimulation intensity of 1.0 V,

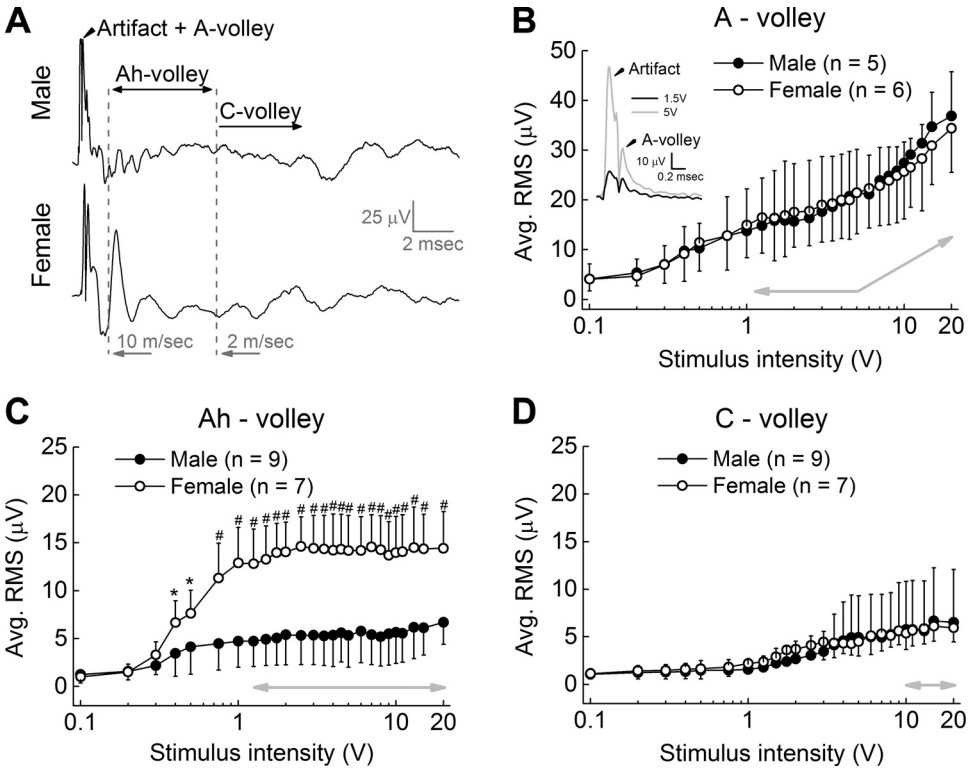

Fig. 4. Ah-type afferent CAP is stable and persistent across suprathreshold stimulus intensities. *A*: representative CAP traces from the aortic depressor nerve (ADN) of male and female rats at high-intensity (20 V) stimulation. Starting at intensities greater than ~5 V, the stimulus artifact extends into the recording epoch associated with A-type fibers (Artifact + A-volley). *B*: as a result, beyond an initial saturation plateau the RMS magnitude of the CAP from the faster conducting (> 10 m/s) A-type fibers increases proportionally with increasing stimulus intensity (note *inset* and gray arrows). *C*: the epochs associated with the CAP arising from the slower-conducting (10–2 m/s) myelinated Ah-type fibers occur well beyond the duration stimulus artifact. As a result, the RMS magnitude of the Ah-volley from female rats is essentially the same magnitude across both low and high stimulation intensities and consistently greater than the Ah-volley from male rat (note horizontal gray arrow). *D*: the RMS magnitude of the much slower (<2 m/s) unmyelinated C-type fibers steadily increased with stimulus intensity until ~10 V, beyond which there was little increase with stimuli up to 20 V. Data are means ± SD. $*P < 0.05$, $\#P < 0.01$.

the average normalized reduction in mean arterial pressure (ΔMAP) from female rats was considerably greater than that from male rats across all but the lowest stimulation frequencies (Fig. 6*A*). As the stimulation intensity increased from 1.0 to 2.0 V, the BRx response in female rats brought about a significantly ($P < 0.01$) greater reduction in ΔMAP than was observed in male rats at nearly every frequency tested between 1 and 100 Hz (Fig. 6, *B* and *C*). Such a strong bias toward significantly greater reductions in the ΔMAP from female rats compared with reductions in ΔMAP from male rats continued through to 3.0 V (data not shown). Beyond 3.0 V of nerve stimulation there continued to be a greater frequency-dependent reduction in ΔMAP in female rats compared with that from male rats, although with an incremental loss in statistical significance as the stimulation intensities approached 5.0 V (Fig. 6*D*).

Baroreflex response profile from selective activation of myelinated baroreceptor afferents. The normalized peak depressor responses (ΔMAP %) for a wide combination of stimulus intensities (1–5 V) and frequencies (1–100 Hz) from all male and female test animals were assembled into 3-dimensional profiles of the integrated BRx response. A linear interpolation unified the data set into a single mesh surface for each sex (Fig. 7, *A* and *B*). Doing so revealed distinct regions within the recruitment profiles that differed considerably between female and male rats. Most apparent were differences at stimulation frequencies in the range of 1–2 Hz, which resulted in a consistent peak reduction in the MAP of ~10% at all but the lowest stimulation intensities (<1.5 V) in female but not in male rats. This trend toward greater evoked depressor response in arterial pressures in female rats continued through to 20 Hz of nerve stimulation. As stimulation frequencies increased toward 100 Hz, the ΔMAP from female rats remained 2- to 10-fold larger than that from male rats although the greatest differences were concentrated within a region of less than ~3.5 V. The numerical difference between these two data profiles revealed a range of stimulus pairs that consistently evoked a much larger reduction in the peak ΔMAP in female compared with male rats (Fig. 7*C*, shaded surface highlights differences greater than 10%). Presented as a 2-dimensional contour plot, the darker (i.e., greater reduction in MAP) regions outline a dynamic operational space within the electrical recruitment profile of myelinated BR fibers that consistently evoked a significantly greater BRx response from female compared with male rats (Fig. 7*D*, dashed box denotes $P < 0.05$). At stimulus intensities just beyond this boundary, the ΔMAP from females remained greater than those observed in males at the same stimulus parameters although not to statistical significance. Beyond ~5.0 V of nerve stimulation there was no apparent difference between the BRx response profiles of male and female rats which presumably involved the graded recruitment of the higher threshold, unmyelinated BR fibers (Fig. 4).

DISCUSSION

Barosensory Ah-type afferent neurons exhibit higher electrical thresholds and broader action potentials with lower rates of sustained somatic discharge compared with A-type (48). At room temperatures, the range of myelinated fiber CV for A- and Ah-type afferent neurons are mostly nonoverlapping (50). Presumably, those fibers exhibiting CV in the range of 10–18 m/s and beyond were the larger A-type, while propagation rates of 4 to ~10 m/s were more typical of Ah-type fibers. Approximately one-third of each population have overlapping CV profiles in the range of 8–16 m/s as well as a small but

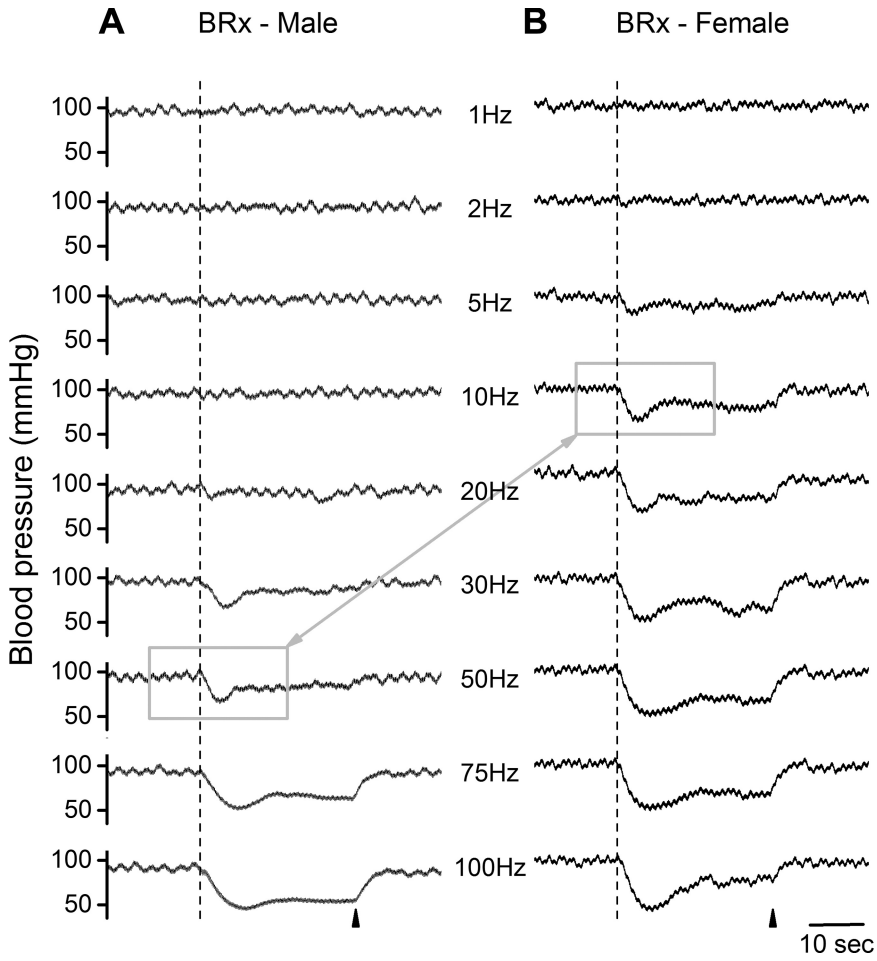

Fig. 5. Bipolar stimulation of the left aortic depressor nerve. A stimulus intensity of 1.5 V provided selective, suprathreshold activation of all A- and Ah-type myelinated fibers (see Fig. 4). This elicited a rapid fall in femoral arterial pressure albeit with unique differences across the depressor responses from male (*A*) and female (*B*) rats. Each trial consisted of a 30-s train of 200-μs monophasic pulses at randomly selected frequencies, arranged here with an ascending order. Dashed line and arrowhead indicate the start and termination, respectively, of nerve stimulation. A depressor response was evident in female rats at stimulation rates as low as 5–10 Hz, well below the nearly 50-Hz stimulation rate required to elicit a comparable peak reduction in femoral mean arterial pressure in male rats (N.B. gray boxes). BRx, baroreflex.

reliable percentage of outliers with signal propagation rates two to three times faster (50).

This study was undertaken to quantify the functional impact such a difference in low-threshold myelinated afferents may have upon the aortic BRx of age-matched female and male Sprague-Dawley rats. Our results offer new perspectives concerning sexual dimorphism in cardiovagal afferent pathways and reflexes, the most notable being: *1*) myelination of BR axons from female rat is, on average, significantly less than that of male rats (Fig. 1); *2*) increasing electrical stimulation of the ADN from subthreshold values provides robust evidence for a second, distinct population of slower conducting myelinated BR fibers in female rats that is not apparent in recordings from male rats (Figs. 2–4); and *3*) the functional impact of this additional population of low-threshold myelinated BR is a significant enhancement of at least the parasympathetic mediated depressor response in female rats (Fig. 5–7). This is most apparent at stimulation magnitudes just sufficient for activation of all myelinated fibers in the ADN. In female rats, a 1.5-V, low-frequency pulse evokes a rapid and robust 20- to 30-mmHg reduction in MAP whereas much greater stimulation frequencies were necessary to evoke a comparable depressor response in male rats.

Myelin area and conduction velocity profiles of the ADN are sexually dimorphic. The rate of action potential propagation in myelinated nerve is markedly influenced by internodal anatomical parameters such as fiber diameter (78). Whether using the long-established quasi-linear relationship between fiber diameter (D) and CV of $1.5 \times D^{1.5}$ (17) or the more simplistic linear scaling of $4.6 \times D$ (7), our in vitro measures of CV for A- and Ah-type afferents of the ADN align quite well with the propagation profiles typical of 1- to 4-μm-diameter Group III sensory afferents and potentially Group II sensory afferents with diameters in the range of 10–12 μm. Such estimates are well within the range of measures from our EM studies where on average total myelin area per BR fiber and the average diameter of myelinated ADN fibers were significantly less in female rats than in male rats.

Calculation of equivalent fiber diameters from measured myelin and axon areas maintained statistical significance, with female rats having on average smaller-diameter myelinated BR fibers (2.33 ± 0.8 vs. 2.45 ± 1.1 μm, $P < 0.05$). As a result, frequency histograms of these estimates of fiber diameter (not shown) had a distribution profile quite consistent with those data presented in Fig. 1, i.e., males trending toward larger magnitudes and females trending toward smaller magnitudes. An extreme example of this trend is evident in the observation that occasionally in male rats, i.e., 3 of 7 ADN tissue samples, there was one myelinated fiber with diameter in the range of 8–12 μm (Fig. 1, *inset*). No such large myelinated fibers were observed in the ADN of female rats. Indeed, in all ADN tissue samples from male rats there were one or more myelinated BR fibers with diameters greater than 6 μm while the largest myelinated BR fiber diameters from female rats never ex-

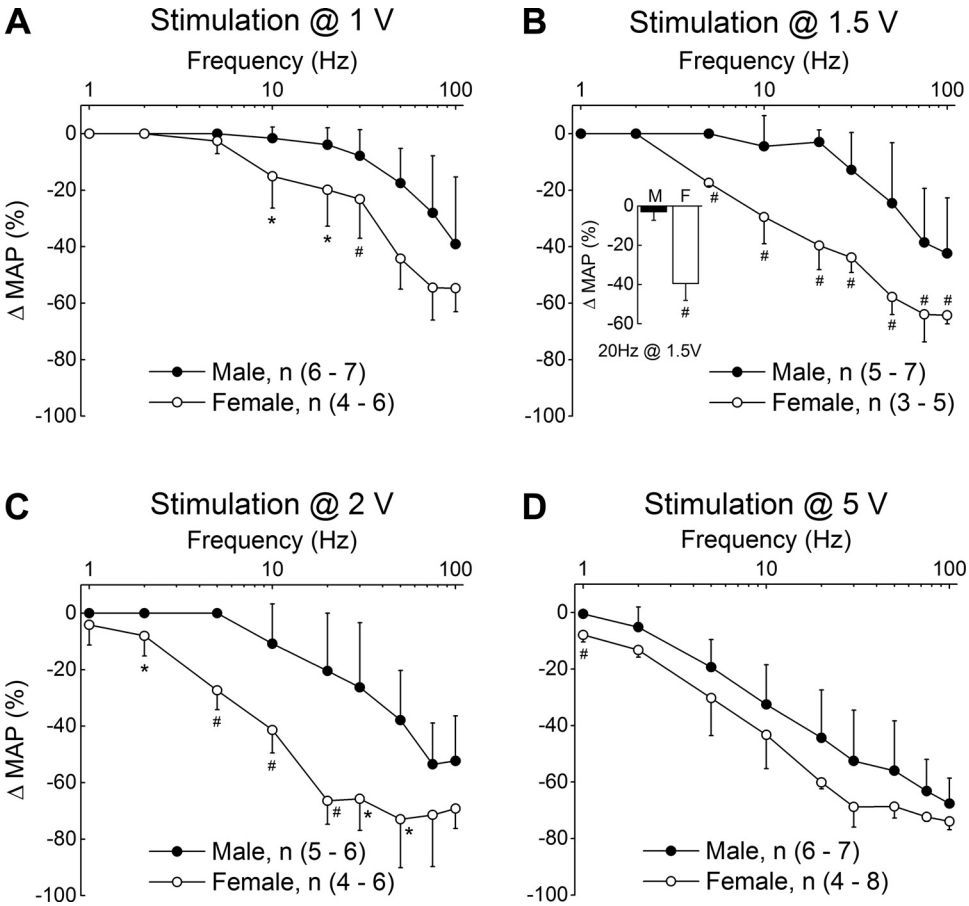

Fig. 6. Average changes in left femoral mean arterial pressure (ΔMAP) evoked through bipolar stimulation of the left ADN using randomly selected pairs of voltage (1–20 V) and frequency (1–100 Hz). *A–C*: low-intensity (≤2 V), low-frequency (≤20 Hz) stimulation of low-threshold myelinated baroreceptor (BR) afferents evoked a substantial depressor reflex in female rats that was essentially lacking in male rats (see *inset*). Stimulation frequencies in excess of 30 Hz were necessary to elicit a comparable reflex response from male rats, although one that was significantly less than that from female rats. *D*: higher intensity (≥5 V) stimulation of the left ADN evoked a depressor reflex of comparable magnitude from male and female rats at all but the lowest rates (≤2 Hz). Results from the nerve conduction studies suggest that beyond ~5 V of nerve stimulation there can be graded recruitment of the higher-threshold, unmyelinated BR afferents (see Figs. 2–4), which bring about a depressor response that is quite similar in male and female rats. Data are means ± SD. $*P < 0.05$, $\#P < 0.01$.

ceeded much more than 5 μm. As a result, the sample distribution of myelin area from females was much more compact, exhibiting a much smaller coefficient of variation than that from males, i.e., 0.70 compared with 1.58, respectively.

To date, morphological measures on ADN fibers from female Sprague-Dawley rats has only been studied by one other laboratory that reported average myelinated fiber diameter and g-ratio values comparable to our data (79). Other investigators have reported similar estimates of myelinated fiber count, diameter, and myelin area, but these studies involved male Wistar-Kyoto, male Wistar-Lewis strains, or pooled measures from both sexes (2, 9, 18, 28). Our study provides statistical support for sexual dimorphism in the myelination of aortic barosensory fibers in Sprague-Dawley rats, an observation that may well extend beyond strain and sensory afferent modality. Evidence for greater myelination of sensory axons of male compared with female rats has been previously reported for other sensory nerves of Long-Evans and Wistar-Kyoto rats (54, 62). Despite a significantly larger-diameter nerve trunk in males than in females ($P < 0.01$), we counted a greater number of myelinated fibers on average per nerve trunk in females than in males, implying a greater packing density for myelinated fibers in female rats. Moore and White (54) made a similar observation for the sensory branches of the pudendal nerve of female Long-Evans rats. Because myelin thickness has a role in determining fiber CV (35, 77), our neuroanatomical data were highly suggestive of potential sex differences in the CV profiles of myelinated aortic barosensory fibers.

Fiber diameter, CV, and discharge threshold for extracellular electrical stimulation are robustly correlated (32, 52, 70). The theory has strong experimental support that larger-diameter myelinated fibers exhibit lower thresholds for extracellular electrical excitation than smaller-diameter myelinated fibers, which require greater stimulus intensities to drive nodal membrane potential toward discharge. Gradual increase of bipolar stimulus intensity brings about a cumulative recruitment of successively smaller myelinated axons within the nerve trunk, increasing the RMS magnitude and duration of the CAP. For both male and female rats and at the lowest intensity tested (0.1 V, top trace in Fig. 2), we detected only the peak corresponding to the lower threshold and presumably larger-diameter A-type barosensory fibers. This fast conducting volley had the shortest latency, making it susceptible to the contaminating effects of the stimulus artifact. In most instances, our recordings from rat ADN exhibited a maximum CV approaching 60 m/s for male and 50 m/s for female rats and always at the lowest stimulus magnitude tested of 0.1 V. Such low threshold and fast conduction speeds in ADN have been reported elsewhere but for larger species such as cat (maximum of 66 m/s) and rabbit (maximum of 40 m/s) (20, 21, 56). Our measured high CV can reasonably be expected to cover the largest-diameter fibers (beyond 8 μm) if utilizing the well-accepted scaling factor of 4.6 (7). Similarly, our selection of a minimum threshold of 10 m/s for CV in assigning afferent fiber type as myelinated A is consistent with estimates of average myelinated fiber diameter for males (2.45 ± 1.1 μm) and age-matched females (2.33 ±

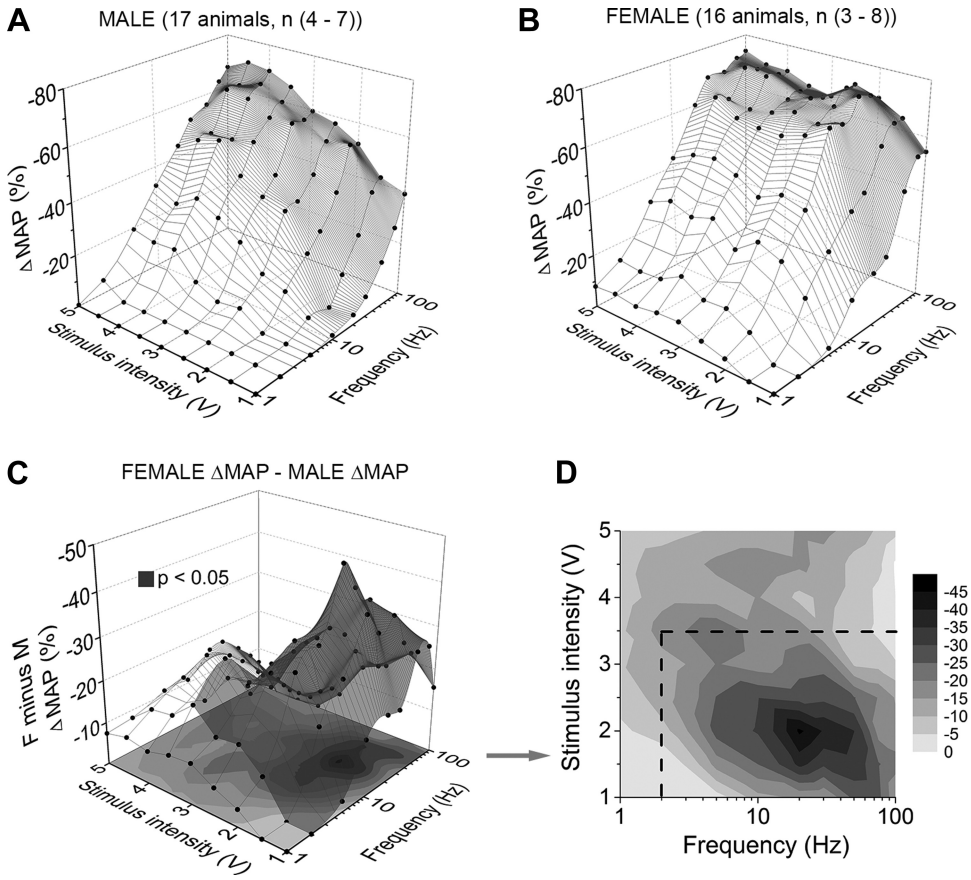

Fig. 7. Peak depressor responses resulting from the selective stimulation of low-threshold, myelinated aortic baroreceptor fibers in male and female rats. Average change in left femoral mean arterial pressure from that just prior to stimulation of the left aortic depressor nerve (ΔMAP) of male (*A*, $n = 17$) and female (*B*, $n = 16$) rats. *C*: absolute difference in the average peak depressor response between male and female rats, i.e., female ΔMAP manifold minus the male ΔMAP manifold, or panel *B* minus panel *A*. The resulting shaded volume highlights the range of low-intensity (1–3.5 V) and low-frequency (peak at 20 Hz) stimulation pairs that evoke a significantly greater depressor responses in female rats than that from male rats. *D*: when presented as a 2-dimensional contour plot the darker areas indicate those pairs of voltage and frequency stimuli that evoke a significantly greater depressor response in females compared with male rats ($P < 0.05$, note the dashed enclosure).

0.8 μm). This estimated lower-limit CV agrees with our lab in vitro electrophysiological (50) data and CV measured in situ by other investigators although the upper limit is highly variable, likely being influenced by stimulus artifact (9, 61).

At slightly higher stimulation intensities but well below the magnitudes necessary for activation of unmyelinated fibers, recruitment of the slower-conducting Ah-type afferents became evident in the myelinated CAP traces of female rats (~0.5 V, 3rd trace from top in Fig. 2). The longer-latency Ah-type CAP component presented with a clear and distinct separation in timing from the faster A-type CAP waveform, although the differences between activation thresholds was quite small, i.e., 0.1 V for A-type and ~0.5 V for Ah-type. This suggests a significant overlap in the distribution of diameters between these two populations of myelinated barosensory fibers in female rats. It is likely that our observations have not been previously reported because the majority of nerve conduction studies performed on the ADN utilize male rats (24, 25, 55). In the few instances where female rats were used, data sets of both sexes were combined, which may account for the slower-conducting myelinated fiber volleys (between 3 and 12 m/s) reported for Wistar-Lewis rats (9). Interestingly, as stimulus intensity increased the Ah-type fiber volley in female rats remained compact and well-defined with stable CV between 8 and 10 m/s. In contrast, males exhibited desynchronized activity that was without a well-defined peak over the same time period (Fig. 2). Such dynamic features of the Ah-type CAP were apparent in the measures of average RMS magnitudes in females which were significantly greater than those from males for all but the lowest stimulation intensities (Figs. 3*B* and 4*C*). Finally, only at stimulus intensities beyond 5 V was there any evidence of recruitment of unmyelinated C-type BR fibers and these CAP profiles had CV well below 2 m/s (Fig. 4*D*). The RMS magnitude of the CAP from A-type and C-type fibers in both sexes was remarkably similar (Figs. 3*A* and 4*D*). Collectively, our neuroanatomical and electrophysiological data indicate that in female rats there exist two functionally distinct myelinated barosensory afferent pathways driving the aortic BRx, whereas only a single and more functionally homogeneous population of myelinated BR fibers is apparent in male rats.

An afferent basis for sexual dimorphism in the aortic baroreceptor reflex. The net effect of BR activation, regardless of the afferent fiber type, is the elevation of the parasympathetic and inhibition of the sympathetic autonomic pathways for cardiovascular control. Our electrophysiological findings showed that thresholds for A- and Ah-type barosensory fibers were typically less than or equal to 0.5 V with maximum recruitment requiring no more than 1.5 V, whereas unmyelinated C-type fibers had discharge thresholds in excess of 5 V (Figs. 2–4). Consequently, low-intensity stimuli of 1.5–3.0 V gave opportunity to investigate selective activation of the myelinated BR afferent pathways without the confounding influence of unmyelinated barosensory fibers upon integrated BRx function. Interestingly, no substantial decreases in MAP were recorded in female or male rats for stimulus intensities below 1 V. This implies that a minimum threshold of barosensory input must be conveyed to the central nervous system to

elicit the BRx mediated depressor response. Our raw BRx response recordings showed new evidence that stimulus intensities as low as 1.5 V elicit a rapid fall in femoral arterial pressure at stimulation rates at or below 10 Hz in female rats, whereas in males similar depressor responses were only achieved at 50 Hz and beyond (Fig. 5). The impact of these observations is apparent in the reflex summary curves, i.e., low-intensity combined with low-frequency (ranging between 1 and 20 Hz) stimulation evoked substantial depressor reflex responses in female rats that were essentially lacking in male rats (Fig. 6). Furthermore, our electrophysiological studies indicated that complete recruitment of A- and Ah-type aortic BR fibers occurs at stimulus intensities close to 2 V (Fig. 3). At this stimulus intensity, activation of A-type volleys in the ADN of male rats evoked reflex changes in MAP only at relatively high frequencies (≥10 Hz) compared with the responses evoked in female rats, which were significantly greater at stimulation rates as low as 2 Hz (Fig. 6*C*). This indicates that the Ah-type BR afferent has a distinctly different frequency range of operation and suggests a functional overlap in the submaximal regions of the A-type afferent frequency-response. Thus, when only the myelinated BR in the ADN are activated, the reflex MAP response in females is elicited over a wider range of frequencies compared with males (Fig. 7*C*). This summation of myelinated afferent subtypes (A + Ah) is responsible for the significantly greater depressor responses in female compared with male rats. Of particular note is a definitive band of low frequencies (<10 to 20 Hz) where at low voltages a robust depressor response is apparent in females but not in male rats. To evoke a comparable fall in MAP of male rats, myelinated fiber discharge across this low frequency band requires the simultaneous recruitment of at least a fraction of the high-threshold unmyelinated barosensory fiber population (Fig. 7).

At elevated stimulus intensities, our typical depressor responses appear to agree with results from Mohamed et al. (53), where a supramaximal stimulus intensity of 30 V was used to activate both A and C fibers in intact, sham-operated, and ovariectomized female rats (53). Here, we focus upon the selective and repeatable graded recruitment of myelinated A- and Ah-type barosensory fibers. One caveat, however, is that the activation of all sensory axons is synchronous. It is unlikely that such a recruitment profile would happen with natural stimuli and therefore it cannot mimic the intrinsic distribution (i.e., multiple and parallel) of sensory inputs to the central nervous system. This must be taken into account when extrapolating our results to an in vivo scenario. Furthermore, we carried out our reflex response studies under anesthesia. The choice of anesthetic can profoundly influence baseline parasympathetic and sympathetic tone, peripheral vascular resistance, as well as the central processing of the BRx. We chose a urethane and α-chloralose cocktail as it has been shown, at the doses used in our experiments, to minimally inhibit the cardiovascular system while providing an adequate depth of anesthesia (39, 69, 76).

Broader implications for sexual dimorphism in cardiovagal function. With such a powerful influence over the cardiovascular system, BR function and dysfunction have been linked to a diverse array of cardiovascular pathologies from acute and chronic hypertension to orthostatic hypotension (OH) (4, 33, 47, 75). Regardless of type, the mechanosensitive terminal ending of a BR fiber neurally encodes a localized pressure-dependent micromechanical distortion of the arterial wall into a frequency-modulated train of action potentials that convey hemodynamic information to the central nervous system. The pressure-discharge attributes of BR fibers have been extensively studied. Myelinated A-type BR or low-threshold pressoreceptors are generally active at normal arterial pressures and produce a regular discharge pattern that faithfully encodes the pressure pulse (14, 42). In stark contrast, unmyelinated C-type BR or high-threshold pressoreceptors require more elevated arterial pressures for activation and exhibit irregular discharge frequencies not well correlated with arterial hemodynamics (73). Although as yet unproven, it is reasonable to speculate that the myelinated Ah-type BR exhibit pressure-discharge properties similar to the A-type BR because they have similar in vitro excitability characteristics, albeit with a slightly higher threshold for activation and lower rates of sustained discharge (48). Our current data support the role of the Ah-type BR afferents as an additional myelinated barosensory pathway to the integrated afferent drive of the BRx. This would imply that for comparable arterial pressures, females but not males exhibit a substantially elevated barosensory input driving centrally mediated BRx pathways. Such an augmented barosensory drive may account for, at least in part, the sex-related differences observed in baseline arterial pressure, cardiovagal BRx, and OH as all implicate a more active parasympathetic control in females compared with males (5, 13, 71).

Although it is not clear which component(s) of the parasympathetic branch of the BRx arc mediates the sex-related differences observed in autonomic reflex function, a BR-mediated elevation in parasympathetic drive is a plausible explanation for the gap in baseline arterial pressure and cardiovagal BRx between the sexes. Emerging evidence shows that healthy young and middle-aged women have lower tonic sympathoadrenal activity-related support of BP (13, 36, 57, 72) and significantly higher parasympathetic markers for heart rate variability compared with age-matched men (8, 46). A BR-mediated elevation in parasympathetic drive along with a concomitant reduction in sympathetic activity could account for, at least in part, the higher resting parasympathetic tone in women compared with men. Likewise, given the potential role of BR in long-term control of MAP (74), a myelinated BR-mediated reduction of sympathetic activity could also be a contributing factor to the lower baseline arterial pressures of premenopausal women, a state often noted as being "cardioprotective" (13, 23).

A recent study by Kim et al. (44) concluded that sex differences in the BRx control of BP appear to be less evident during BR unloading, i.e., simulated hypotension, than BR loading, i.e., simulated hypertension. In response to the latter, women exhibited "an exaggerated reduction in BP compared to men" (29). Broadly, such observations are in agreement with our experimental results in that electrical stimulation of the ADN, i.e., elevating barosensory fiber discharge as consistent with a hypertensive event, results in greater hypotensive responses in female compared with male rats. Also noteworthy are studies implicating that the hemodynamic capacity to compensate for postural changes from a supine to an upright position is greater in men than in women (5, 16). Such OH can manifest with extreme symptoms such as vasovagal or reflex syncope (11) ensuing an abrupt fall in systemic BP (12). Differences in body size and contributing factors such as sex

hormones and genetics do not explain the sex bias observed in OH between the sexes (12, 30). Because orthostatic BP regulation in women occurs via parasympathetic withdrawal more than sympathetic activation (3, 34), a BR-mediated increase in tonic resting parasympathetic activity could result in women requiring a larger increase in HR compared with men to achieve orthostatic stabilization.

Summary and perspectives. The differential myelination of aortic BR fibers of male and female rats gives rise to sexually dimorphic recruitment patterns of the myelinated afferent fibers. Only female rats consistently exhibited an additional myelinated fiber volley corresponding to low-threshold Ah-type BR fibers. In situ BRx experiments demonstrated that the functional contributions of this myelinated barosensory afferent pathway bring about greater BRx responses in females compared with males at lower frequencies than previously reported for stimulus specific for myelinated fiber activation. Collectively, our findings suggest that in vivo the physiological role of the Ah-type BR afferents is to mediate the low-pressure threshold drive of the BRx, potentially providing an enhanced parasympathetic control of BP in females compared with males. Although we did not resolve the independent contributions of Ah-type BR fibers to BRx function, our result are consistent with the hypothesis that Ah-type BR afferents contribute to the sexual dimorphism observed in basal autonomic BRx function. As such, the "cardioprotection" observed in premenopausal women may be linked to this sex-specific BR afferent. Since sex hormones have been suggested to serve a neuromodulatory role, correlative nerve conduction and BRx studies in intact vs. ovariectomized female rats could help clarify the impact of ovarian sex steroids on BR afferent function. Finally, aortic BR form part of a larger population of multimodal vagal sensory neurons which also show sexual dimorphism in the functional expression of Ah-type myelinated afferents (48, 60). Consequently, our findings may offer alternative explanations for disorders associated with vagal afferent function and dysfunction such as irritable bowel syndrome and other disorders of the viscera.

GRANTS

This work was supported by National Institutes of Health Grants HL-072012 and HL-081819 to J. H. Schild with an administrative supplement to G. Santa Cruz Chavez.

DISCLOSURES

No conflicts of interest, financial or otherwise, are declared by the author(s).

AUTHOR CONTRIBUTIONS

Author contributions: G.C.S.C.C. and P.A.G. performed experiments; G.C-.S.C.C., B.-Y.L., and J.H.S. analyzed data; G.C.S.C.C. and J.H.S. interpreted results of experiments; G.C.S.C.C. and J.H.S. prepared figures; G.C.S.C.C. and J.H.S. drafted manuscript; G.C.S.C.C., D.L.K., and J.H.S. edited and revised manuscript; G.C.S.C.C., B.-Y.L., P.A.G., D.L.K., and J.H.S. approved final version of manuscript; J.H.S. conception and design of research.

REFERENCES

1. **Andresen MC, Doyle MW, Bailey TW, Jin YH.** Differentiation of autonomic reflex control begins with cellular mechanisms at the first synapse within the nucleus tractus solitarius. *Br J Med Biol Res* 37: 549–558, 2004.
2. **Andresen MC, Krauhs JM, Brown AM.** Relationship of aortic wall and baroreceptor properties during development in normotensive and spontaneously hypertensive rats. *Circ Res* 43: 728–738, 1978.
3. **Arzeno NM, Stenger MB, Lee SM, Ploutz-Snyder R, Platts SH.** Sex differences in blood pressure control during 6 degrees head-down tilt bed rest. *Am J Physiol Heart Circ Physiol* 304: H1114–H1123, 2013.
4. **Aung T, Fan W, Krishnamurthy M.** Recurrent syncope, orthostatic hypotension and volatile hypertension: think outside the box. *J Community Hosp Intern Med Perspect* 3, 2013.
5. **Barantke M, Krauss T, Ortak J, Lieb W, Reppel M, Burgdorf C, Pramstaller PP, Schunkert H, Bonnemeier H.** Effects of gender and aging on differential autonomic responses to orthostatic maneuvers. *J Cardiovasc Electrophysiol* 19: 1296–1303, 2008.
6. **Beske SD, Alvarez GE, Ballard TP, Davy KP.** Gender difference in cardiovagal baroreflex gain in humans. *J Appl Physiol* 91: 2088–2092, 2001.
7. **Boyd IA, Kalu KU.** Scaling factor relating conduction velocity and diameter for myelinated afferent nerve fibres in the cat hind limb. *J Physiol* 289: 277–297, 1979.
8. **Britton A, Shipley M, Malik M, Hnatkova K, Hemingway H, Marmot M.** Changes in heart rate and heart rate variability over time in middle-aged men and women in the general population (from the Whitehall II Cohort Study). *Am J Cardiol* 100: 524–527, 2007.
9. **Brown AM, Saum WR, Tuley FH.** A comparison of aortic baroreceptor discharge in normotensive and spontaneously hypertensive rats. *Circ Res* 39: 488–496, 1976.
10. **Brown AM, Saum WR, Yasui S.** Baroreceptor dynamics and their relationship to afferent fiber type and hypertension. *Circ Res* 42: 694–702, 1978.
11. **Chen-Scarabelli C, Scarabelli TM.** Neurocardiogenic syncope. *BMJ* 329: 336–341, 2004.
12. **Cheng YC, Vyas A, Hymen E, Perlmuter LC.** Gender differences in orthostatic hypotension. *Am J Med Sci* 342: 221–225, 2011.
13. **Christou DD, Jones PP, Jordan J, Diedrich A, Robertson D, Seals DR.** Women have lower tonic autonomic support of arterial blood pressure and less effective baroreflex buffering than men. *Circulation* 111: 494–498, 2005.
14. **Coleridge HM, Coleridge JC.** Cardiovascular afferents involved in regulation of peripheral vessels. *Annu Rev Physiol* 42: 413–427, 1980.
15. **Conte MR.** Gender differences in the neurohumoral control of the cardiovascular system. *Ital Heart J* 4: 367–370, 2003.
16. **Convertino VA.** Gender differences in autonomic functions associated with blood pressure regulation. *Am J Physiol Regul Integr Comp Physiol* 275: R1909–R1920, 1998.
17. **Coppin CM, Jack JJ.** Internodal length and conduction velocity of cat muscle afferent nerve fibres. *J Physiol* 222: 92P–93P, 1972.
18. **da Silva AP, Jordao CE, Fazan VP.** Peripheral nerve morphometry: comparison between manual and semi-automated methods in the analysis of a small nerve. *J Neurosci Methods* 159: 153–157, 2007.
19. **Dart AM, Du XJ, Kingwell BA.** Gender, sex hormones and autonomic nervous control of the cardiovascular system. *Cardiovasc Res* 53: 678–687, 2002.
20. **Devanandan MS.** A study of the myelinated fibres of the aortic nerve of cats. *J Physiol* 171: 361–367, 1964.
21. **Douglas WW, Ritchie JM, Schaumann W.** Depressor reflexes from medullated and non-medullated fibres in the rabbits aortic nerve. *J Physiol* 132: 187–198, 1956.
22. **Du XJ, Dart AM, Riemersma RA.** Sex differences in the parasympathetic nerve control of rat heart. *Clin Exp Pharmacol Physiol* 21: 485–493, 1994.
23. **Fallen EL.** Vagal afferent stimulation as a cardioprotective strategy? Introducing the concept. *Ann Noninvasive Electrocardiol* 10: 441–446, 2005.
24. **Fan W, Andresen MC.** Differential frequency-dependent reflex integration of myelinated and nonmyelinated rat aortic baroreceptors. *Am J Physiol Heart Circ Physiol* 275: H632–H640, 1998.
25. **Fan W, Reynolds PJ, Andresen MC.** Baroreflex frequency-response characteristics to aortic depressor and carotid sinus nerve stimulation in rats. *Am J Physiol Heart Circ Physiol* 271: H2218–H2227, 1996.
26. **Fan W, Schild JH, Andresen MC.** Graded and dynamic reflex summation of myelinated and unmyelinated rat aortic baroreceptors. *Am J Physiol Regul Integr Comp Physiol* 277: R748–R756, 1999.
27. **Fazan PV, Junior FR, Salgado CH, Barreira AA.** Morphology of aortic depressor nerve myelinated fibers in normotensive Wistar-Kyoto and spontaneously hypertensive rats. *J Auton Nerv Syst* 77: 133–139, 1999.

28. **Fazan VP, Salgado HC, Barreira AA.** A descriptive and quantitative light and electron microscopy study of the aortic depressor nerve in normotensive rats. *Hypertension* 30: 693–698, 1997.
29. **Fisher JP, Kim A, Hartwich D, Fadel PJ.** New insights into the effects of age and sex on arterial baroreflex function at rest and during dynamic exercise in humans. *Auton Neurosci* 172: 13–22, 2012.
30. **Franke WD, Johnson CP, Steinkamp JA, Wang R, Halliwill JR.** Cardiovascular and autonomic responses to lower body negative pressure: do not explain gender differences in orthostatic tolerance. *Clin Auton Res* 13: 36–44, 2003.
31. **Glick G, Braunwald E.** Relative roles of the sympathetic and parasympathetic nervous systems in the reflex control of heart rate. *Circ Res* 16: 363–375, 1965.
32. **Gorman PH, Mortimer JT.** The effect of stimulus parameters on the recruitment characteristics of direct nerve stimulation. *IEEE Trans Biomed Eng* 30: 407–414, 1983.
33. **Grassi G, Cattaneo BM, Seravalle G, Lanfranchi A, Mancia G.** Baroreflex control of sympathetic nerve activity in essential and secondary hypertension. *Hypertension* 31: 68–72, 1998.
34. **Harm DL, Jennings RT, Meck JV, Powell MR, Putcha L, Sams CP, Schneider SM, Shackelford LC, Smith SM, Whitson PA.** Gender issues related to spaceflight: a NASA perspective. *J Appl Physiol (1985)* 91: 2374–2383, 2001.
35. **Harper AA, Lawson SN.** Conduction velocity is related to morphological cell type in rat dorsal root ganglion neurones. *J Physiol* 359: 31–46, 1985.
36. **Hogarth AJ, Mackintosh AF, Mary DA.** Gender-related differences in the sympathetic vasoconstrictor drive of normal subjects. *Clin Sci (Lond)* 112: 353–361, 2007.
37. **Huikuri HV, Pikkujamsa SM, Airaksinen KE, Ikaheimo MJ, Rantala AO, Kauma H, Lilja M, Kesaniemi YA.** Sex-related differences in autonomic modulation of heart rate in middle-aged subjects. *Circulation* 94: 122–125, 1996.
38. **Huxley VH.** Sex and the cardiovascular system: the intriguing tale of how women and men regulate cardiovascular function differently. *Adv Physiol Educ* 31: 17–22, 2007.
39. **Jackson DN, Noble EG, Shoemaker JK.** Y1- and alpha1-receptor control of basal hindlimb vascular tone. *Am J Physiol Regul Integr Comp Physiol* 287: R228–R233, 2004.
40. **Jin YH, Bailey TW, Li BY, Schild JH, Andresen MC.** Purinergic and vanilloid receptor activation releases glutamate from separate cranial afferent terminals in nucleus tractus solitarius. *J Neurosci* 24: 4709–4717, 2004.
41. **Kardon MB, Peterson DF, Bishop VS.** Reflex heart rate control via specific aortic nerve afferents in the rabbit. *Circ Res* 37: 41–47, 1975.
42. **Katona PG, Poitras JW, Pantelakis N, Jensen EW, Barnett GO.** Deterministic nature of baroreceptor firing. *Am J Physiol* 215: 1–7, 1968.
43. **Kim A, Deo SH, Fisher JP, Fadel PJ.** Effect of sex and ovarian hormones on carotid baroreflex resetting and function during dynamic exercise in humans. *J Appl Physiol (1985)* 112: 1361–1371, 2012.
44. **Kim A, Deo SH, Vianna LC, Balanos GM, Hartwich D, Fisher JP, Fadel PJ.** Sex differences in carotid baroreflex control of arterial blood pressure in humans: relative contribution of cardiac output and total vascular conductance. *Am J Physiol Heart Circ Physiol* 301: H2454–H2465, 2011.
45. **Kobayashi M, Cheng ZB, Tanaka K, Nosaka S.** Is the aortic depressor nerve involved in arterial chemoreflexes in rats? *J Auton Nerv Syst* 78: 38–48, 1999.
46. **Kuch B, Hense HW, Sinnreich R, Kark JD, von Eckardstein A, Sapoznikov D, Bolte HD.** Determinants of short-period heart rate variability in the general population. *Cardiology* 95: 131–138, 2001.
47. **La Rovere MT, Pinna GD, Maestri R, Sleight P.** Clinical value of baroreflex sensitivity. *Neth Heart J* 21: 61–63, 2013.
48. **Li BY, Qiao GF, Feng B, Zhao RB, Lu YJ, Schild JH.** Electrophysiological and neuroanatomical evidence of sexual dimorphism in aortic baroreceptor and vagal afferents in rat. *Am J Physiol Regul Integr Comp Physiol* 295: R1301–R1310, 2008.
49. **Li BY, Schild JH.** Comparisons of somatic action potentials from dispersed and intact rat nodose ganglia using patch-clamp technique. *Acta Pharmacol Sin* 23: 481–489, 2002.
50. **Li BY, Schild JH.** Electrophysiological and pharmacological validation of vagal afferent fiber type of neurons enzymatically isolated from rat nodose ganglia. *J Neurosci Methods* 164: 75–85, 2007.
51. **Maranon R, Reckelhoff JF.** Sex and gender differences in control of blood pressure. *Clin Sci (Lond)* 125: 311–318, 2013.
52. **McNeal DR.** Analysis of a model for excitation of myelinated nerve. *IEEE Trans Biomed Eng* 23: 329–337, 1976.
53. **Mohamed MK, El-Mas MM, Abdel-Rahman AA.** Estrogen enhancement of baroreflex sensitivity is centrally mediated. *Am J Physiol Regul Integr Comp Physiol* 276: R1030–R1037, 1999.
54. **Moore CL, White RH.** Sex differences in sensory and motor branches of the pudendal nerve of the rat. *Horm Behav* 30: 590–599, 1996.
55. **Numao Y, Siato M, Terui N, Kumada M.** The aortic nerve-sympathetic reflex in the rat. *J Auton Nerv Syst* 13: 65–79, 1985.
56. **Paintal AS.** The conduction velocities of respiratory and cardiovascular afferent fibres in the vagus nerve. *J Physiol* 121: 341–359, 1953.
57. **Peckerman A, Hurwitz BE, Nagel JH, Leitten C, Agatston AS, Schneiderman N.** Effects of gender and age on the cardiac baroreceptor reflex in hypertension. *Clin Exp Hypertens* 23: 645–656, 2001.
58. **Perge JA, Niven JE, Mugnaini E, Balasubramanian V, Sterling P.** Why do axons differ in caliber? *J Neurosci* 32: 626–638, 2012.
59. **Pickering TG, Davies J.** Estimation of the conduction time of the baroreceptor-cardiac reflex in man. *Cardiovasc Res* 7: 213–219, 1973.
60. **Qiao GF, Li BY, Lu YJ, Fu YL, Schild JH.** 17Beta-estradiol restores excitability of a sexually dimorphic subset of myelinated vagal afferents in ovariectomized rats. *Am J Physiol Cell Physiol* 297: C654–C664, 2009.
61. **Reynolds PJ, Fan W, Andresen MC.** Capsaicin-resistant arterial baroreceptors. *J Negat Results Biomed* 5: 6, 2006.
62. **Sanada LS, da Rocha Kalil AL, Tavares MR, Neubern MC, Salgado HC, Fazan VP.** Sural nerve involvement in experimental hypertension: morphology and morphometry in male and female normotensive Wistar-Kyoto (WKY) and spontaneously hypertensive rats (SHR). *BMC Neurosci* 13: 24, 2012.
63. **Sapru HN, Gonzalez E, Krieger AJ.** Aortic nerve stimulation in the rat: cardiovascular and respiratory responses. *Brain Res Bull* 6: 393–398, 1981.
64. **Schild JH, Kunze DL.** Differential distribution of voltage-gated channels in myelinated and unmyelinated baroreceptor afferents. *Auton Neurosci* 172: 4–12, 2012.
65. **Schneider CA, Rasband WS, Eliceiri KW.** NIH Image to ImageJ: 25 years of image analysis. *Nat Methods* 9: 671–675, 2012.
66. **Seagard JL, Hopp FA, Drummond HA, Van Wynsberghe DM.** Selective contribution of two types of carotid sinus baroreceptors to the control of blood pressure. *Circ Res* 72: 1011–1022, 1993.
67. **Simms AE, Paton JF, Pickering AE.** Hierarchical recruitment of the sympathetic and parasympathetic limbs of the baroreflex in normotensive and spontaneously hypertensive rats. *J Physiol* 579: 473–486, 2007.
68. **Smetana P, Malik M.** Sex differences in cardiac autonomic regulation and in repolarisation electrocardiography. *Pflügers Arch* 465: 699–717, 2013.
69. **Stornetta RL, Guyenet PG, McCarty RC.** Autonomic nervous system control of heart rate during baroreceptor activation in conscious and anesthetized rats. *J Auton Nerv Syst* 20: 121–127, 1987.
70. **Sundar S, Gonzalez-Cueto J.** Selective activation of small nerve fibers for assessing carpal tunnel syndrome. *Conf Proc IEEE Eng Med Biol Soc* 4: 3668–3671, 2005.
71. **Tanaka M, Sato M, Umehara S, Nishikawa T.** Influence of menstrual cycle on baroreflex control of heart rate: comparison with male volunteers. *Am J Physiol Regul Integr Comp Physiol* 285: R1091–R1097, 2003.
72. **Tank J.** Does aging cause women to be more sympathetic than men? *Hypertension* 45: 489–490, 2005.
73. **Thoren P, Saum WR, Brown AM.** Characteristics of rat aortic baroreceptors with nonmedullated afferent nerve fibers. *Circ Res* 40: 231–237, 1977.
74. **Thrasher TN.** Arterial baroreceptor input contributes to long-term control of blood pressure. *Curr Hypertens Rep* 8: 249–254, 2006.
75. **Ufnal M.** Essential hypertension—is erroneous receptor output to blame? *Med Hypotheses* 78: 454–458, 2012.
76. **Usselman CW, Mattar L, Twynstra J, Welch I, Shoemaker JK.** Rodent cardiovascular responses to baroreceptor unloading: effect of plane of anaesthesia. *Appl Physiol Nutr Metab* 36: 376–381, 2011.
77. **Waxman SG.** Determinants of conduction velocity in myelinated nerve fibers. *Muscle Nerve* 3: 141–150, 1980.
78. **Waxman SG, Kocsis JD, Stys PK.** *The Axon: Structure, Function and Pathophysiology*. New York, NY: Oxford University Press, 1995.
79. **Yamasaki M, Shimizu T, Katahira K, Waki H, Nagayama T, HOI, Katsuda S, Miyake M, Miyamoto Y, Wago H, Okouchi T, Matsumoto S.** Spaceflight alters the fiber composition of the aortic nerve in the developing rat. *Neuroscience* 128: 819–829, 2004.